Parameter Estimation of Three-Phase Untransposed Short Transmission Lines from Synchrophasor Measurements

Antoine Wehenkel, Arpan Mukhopadhyay, Jean-Yves Le Boudec and Mario Paolone

***Abstract*—We present a new approach for estimating the parameters of three-phase untransposed electrically short transmission lines using voltage/current synchrophasor measurements obtained from phasor measurement units. The parameters to be estimated are the entries of the longitudinal impedance matrix and the shunt admittance matrix at the rated system frequency. Conventional approaches relying on the admittance matrix of the line cannot accurately estimate these parameters for short lines, due to their high sensitivity to measurement noise. Our approach differs from the conventional ones in the following ways: First, we model the line by the three-phase transmittance matrix that is observed to be less sensitive to measurement noise than the admittance matrix. Second, we compute an accurate noise covariance matrix using the realistic specifications of noise introduced by instrument transformers and phasor measurement units. This noise covariance matrix is then used in least-squares-based estimation methods. Third, we derive different least-squares-based estimation methods based on a statistical model of estimation and show that the weighted least-squares and the maximum likelihood methods, which make use of the noise covariance matrix produce the best estimates of the line parameters. Finally, we apply the proposed methods to a real dataset and show that our approach significantly outperforms existing ones.**

I. Introduction

Fundamental functionalities used in the operation of power grids, e.g., state estimation (SE) [1], [2], [3], optimal power flow (OPF)-based control [4], [5], [6], [7], , Model Predictive Control [8], [9] and optimal relay tuning [10], [11], require the knowledge of transmission line (TL) parameters at the rated system frequency. Conventionally, TL parameters are obtained either by using the physical properties of the line (such as conductor dimensions, types of wires, tower geometries, ground electrical parameters) [12], [13] or by making measurements on the line when it is off-grid [14]. The first method is applicable only when accurate conductor characteristics are known, whereas the second method, although reliable, is time consuming and difficult to implement in practice.

With the availability of highly accurate measurement devices, e.g., phasor measurement units (PMUs), instrument transformers (ITs), estimation methods based on measurements from these devices have gained significant research attention [15], [16], [17], [18], [19], [20]. PMUs, along with ITs, are used to obtain time-synchronous phasor measurements of nodal phase-to-ground voltages and terminal currents at both ends of a TL. These measurements can be used to estimate the parameters of the TL.

The use of the total least-squares (TLS) technique for estimating TL parameters is proposed in [17]. [21] and [22] propose methods for eliminating systematic errors introduced by ITs into the measurements. However, these methods assume the TLs to be fully transposed and symmetric. For untransposed, non-symmetric TLs, [23] proposes an estimation method based on ordinary least-squares (OLS). However, as reported in [24], the method requires prior knowledge of the ranges of the parameters to have an acceptable accuracy of estimation and to avoid the presence of outliers in the data. A robust method for estimating three-phase parameters of untransposed lines is proposed in [25], where the main focus is to reduce the effect bad-data or outliers without the need for separate bad-data detection algorithms. Recently, a method based on trimmed least squares techniques has been proposed for parameters estimation of TLs from data measured in single pole open conditions. Concurrently, PMU based parameters estimations have been proposed for distribution networks [16], the estimation problem in this context can be considered as easier due to the higher variability in the data of an operating distribution network compared to the one observed in the operating transmission networks. The use of Kalman filtering is proposed in [26]. It improves the estimation accuracy in comparison to the least-squares based methods. All works mentioned above use line models that are highly sensitive to measurement noise. Consequently, the accuracy of these methods deteriorates significantly when applied to short transmission lines that have smaller parameter values and are therefore more sensitive to noise. Furthermore, all prior works lack a realistic noise model (that captures the characteristics of real PMUs and ITs) and do not account for the effects of realistic loading condition of the grid on parameter estimation. Hence, their results are of limited use.

Contributions: Our main contributions are (i) the use of a new line model for estimation, (ii) the derivation of an accurate noise covariance matrix from realistic specifications of the measurement devices, (iii) derivation of different estimation methods from a statistical model of estimation, and (iv) application of these methods to a real dataset that captures the effect of different loading conditions of the grid to show the efficacy of the methods. The detailed contributions are given

A. Wehenkel is with the Department of Electrical Engineering and Computer Science, University of Liege, Belgium, and is supported by the Fund for Scientific Research (FNRS). e-mail: antoine.wehenkel@uliege.be

A. Mukhopadhyay is with the Department of Computer Science, University of Warwick, UK.

J. Y. Le Boudec, and M. Paolone are with École Polytechnique Fédérale de Lausanne (EPFL), 1015 Lausanne, Switzerland.

below:

(1) *Line modeling:* All existing methods for TL parameter estimation fail for short lines, due to their high noise sensitivity. To overcome this difficulty, we propose a model based on the transmittance matrix of the line. We compare the proposed model with other line models that use the impedance and admittance matrices. The comparison is achieved both by directly estimating the line parameters under different line models and by comparing the Cramer-Rao bounds (CRBs) that correspond to these models. We observe that the proposed model has the least noise sensitivity among all models for short lines.

(2) *Noise modeling*: We use an accurate statistical model for measurement noise. The model is based on realistic specifications of ITs and PMUs. Since the specifications are made in polar coordinates, we transform them to rectangular coordinates to compute the noise covariance matrix which is then used by different estimation methods. This accurate characterization of the measurement noise makes our results more practicable than existing ones. Furthermore, we observe that including the noise covariance matrix in our estimation methods results in reduced estimation errors.

(3) *Estimation methods*: We evaluate the performance of several estimation methods that differ in their likelihood functions. The likelihood functions are derived from our statistical model and give rise to different least-squares based estimation methods. We compare the performance of OLS, weighted least-squares (WLS), TLS, and maximum likelihood (ML) estimators. We show that the WLS and the ML estimators are the most accurate ones among all as they make use of the noise covariance matrices discussed above.

(4) *Use of realistic data*: We evaluate all our methods by estimating the parameters of short transmission lines used in a real high voltage (HV) sub-transmission grid. The values of voltages and currents are also taken from a real data-set containing the values of these quantities for an entire day of operation of the above mentioned grid. Thus, unlike previous works, our results incorporate the effect of different loading conditions of the grid. We observe that with our proposed approach the line parameters are estimated with high accuracy.

Although our main focus in the paper is on estimating parameters of short lines, we observe that our approach produces accurate estimates of line parameters for all line lengths. In fact, estimating the parameters for longer lines turns out to be significantly easier than estimating parameters for short lines due to the reduced effect of measurement noise in the former case. In case of long lines, we observe that models based on either the impedance or the admittance matrix representations of the lines, in conjunction with the proposed methods, can accurately recover the line parameters.

The rest of the paper is organized as follows. In Section II, we formulate the problem of line-parameter estimation by using different line models and introduce the noise model used in the paper. In Section III, we describe the proposed estimation methods. In Section IV, we numerically evaluate the performance of the proposed methods. We conclude the paper in Section V.

Some Notations: We use $\mathbb{C}$ and $\mathbb{R}$ to denote the set of complex and real numbers, respectively; matrices are written using bold symbols; for a matrix $\mathbf{M}$ the $(i,j)^{\text{th}}$ entry is denoted by $(\mathbf{M})_{ij}$; vectors are column vectors unless specified otherwise; $'$ denotes transpose; $\mathcal{R}(w)$ and $\mathcal{I}(w)$ denote the real and imaginary parts of a complex vector w, respectively; $\mathsf{diag}(\mathbf{X}_1,\ldots,\mathbf{X}_n)$ denotes the the block-diagonal matrix with $\mathbf{X}_i$, $i=1:n$, as its blocks. We use the generic notation θ for an unknown parameter vector of dimension $\mathcal{S}_\theta$ and $\hat{\theta}$ to denote its estimate.

II. Problem Formulation

We are interested in identifying the entries of the longitudinal impedance and shunt admittance matrices at the rated system frequency of an untransposed three-phase line modelled via its π equivalent circuit (see Figure 1). Let the three-phase longitudinal impedance and shunt admittance matrices of a line between the two nodes s and r be denoted by $\mathbf{Z}_l \in \mathbb{C}^{3\times 3}$ and $\mathbf{Y}_l \in \mathbb{C}^{3\times 3}$, respectively. Let $v^x, i^x \in \mathbb{C}^3$ denote the complex nodal phase-to-ground voltage and terminal current at node $x \in \{s,r\}$, respectively. The objective is to estimate the entries of $\mathbf{Y}_l$ and $\mathbf{Z}_l$ from noisy measurements of i^x and v^x obtained from PMUs. To do so, we first need to express the relationship among the phasors and the line parameters by using a line model. Below, we discuss several line models, each of which leads to a different estimation problem. A comparison of these models, in terms of estimation accuracy, is provided later.

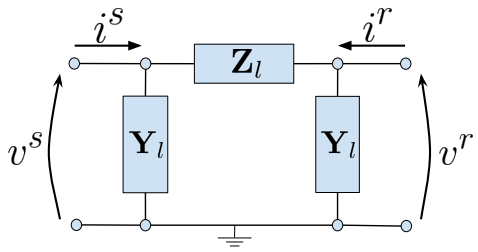

Fig. 1. Equivalent π-model of a three-phase TL

A. Transmittance Matrix Model

With the transmittance matrix, the relationship between the phasors and line parameters can be expressed as follows [27]:

$$\begin{bmatrix} v^s \\ i^s \end{bmatrix} = \begin{bmatrix} \mathbf{I} + \frac{\mathbf{Z}_l\mathbf{Y}_l}{2} & -\mathbf{Z}_l \\ \mathbf{Y}_l\left(\mathbf{I} + \frac{\mathbf{Z}_l\mathbf{Y}_l}{4}\right) & -\left(\mathbf{I} + \frac{\mathbf{Y}_l\mathbf{Z}_l}{2}\right) \end{bmatrix} \begin{bmatrix} v^r \\ i^r \end{bmatrix}, \quad (1)$$

$$\approx \begin{bmatrix} \mathbf{I} & -\mathbf{Z}_l \\ \mathbf{Y}_l & -\mathbf{I} \end{bmatrix} \begin{bmatrix} v^r \\ i^r \end{bmatrix}, \quad (2)$$

where $\mathbf{I} \in \mathbb{C}^{3\times 3}$ denotes the complex identity matrix. The approximation in (2) is obtained by using the fact that the product matrix $\mathbf{Z}_l\mathbf{Y}_l$ is usually very close to the null matrix $\mathbf{0} \in \mathbb{C}^{3\times 3}$ for lines that are electrically short (i.e. < 80km, e.g. [28]), i.e., $\mathbf{Z}_l\mathbf{Y}_l \approx \mathbf{0}$. We refer to this approximation as the 'short-line approximation' and have verified that the approximation is accurate for short lines and some medium

length lines($<$ 200km), operating at very high rated voltages (e.g., 380 kV). We refer to the line model expressed by (2) as the T-line model.

To obtain a linear estimation model, we need to express the T-line model as a linear function of the unknown parameters. The most generic parameterization using an unknown vector $\theta^{\mathbf{T}} = [\theta_1^{\mathbf{T}}, ..., \theta_{24}^{\mathbf{T}}]' \in \mathbb{R}^{24}$ in 24 dimensions is given below

$$\mathbf{Y}_l(\theta^{\mathbf{T}}) = \begin{bmatrix} \theta_{19}^{\mathbf{T}} \theta_{22}^{\mathbf{T}} \theta_{23}^{\mathbf{T}} \\ \theta_{22}^{\mathbf{T}} \theta_{20}^{\mathbf{T}} \theta_{24}^{\mathbf{T}} \\ \theta_{23}^{\mathbf{T}} \theta_{24}^{\mathbf{T}} \theta_{21}^{\mathbf{T}} \end{bmatrix} + j \begin{bmatrix} \theta_1^{\mathbf{T}} \theta_{16}^{\mathbf{T}} \theta_{17}^{\mathbf{T}} \\ \theta_{16}^{\mathbf{T}} \theta_2^{\mathbf{T}} \theta_{18}^{\mathbf{T}} \\ \theta_{17}^{\mathbf{T}} \theta_{18}^{\mathbf{T}} \theta_3^{\mathbf{T}} \end{bmatrix}, \tag{3}$$

$$\mathbf{Z}_l(\theta^{\mathbf{T}}) = \begin{bmatrix} \theta_4^{\mathbf{T}} \theta_6^{\mathbf{T}} \theta_8^{\mathbf{T}} \\ \theta_6^{\mathbf{T}} \theta_{10}^{\mathbf{T}} \theta_{12}^{\mathbf{T}} \\ \theta_8^{\mathbf{T}} \theta_{12}^{\mathbf{T}} \theta_{14}^{\mathbf{T}} \end{bmatrix} + j \begin{bmatrix} \theta_5^{\mathbf{T}} \theta_7^{\mathbf{T}} \theta_9^{\mathbf{T}} \\ \theta_7^{\mathbf{T}} \theta_{11}^{\mathbf{T}} \theta_{13}^{\mathbf{T}} \\ \theta_9^{\mathbf{T}} \theta_{13}^{\mathbf{T}} \theta_{15}^{\mathbf{T}} \end{bmatrix}, \tag{4}$$

where the $\mathbf{T}$ in the superscript of $\theta^{\mathbf{T}}$ indicates that it is a parameterization of the T-line model. Using the parameterization above, we can rewrite (2) after separating the real and imaginary parts as follows:

$$l_{\mathbf{T}}^s = \bar{\mathbf{T}}(\theta^{\mathbf{T}}) l_{\mathbf{T}}^r = \mathbf{H}_{\mathbf{T}}(l_{\mathbf{T}}^r)\theta^{\mathbf{T}} + \gamma_{\mathbf{T}}(l_{\mathbf{T}}^r), \tag{5}$$

where for $x \in \{r, s\}$

$$l_{\mathbf{T}}^x = \begin{bmatrix} \mathcal{R}(v^x) \\ \mathcal{R}(i^x) \\ \mathcal{I}(v^x) \\ \mathcal{I}(i^x) \end{bmatrix} \in \mathbb{R}^{12}, \quad \gamma_{\mathbf{T}}(l_{\mathbf{T}}^x) = \begin{bmatrix} \mathbf{I} & \mathbf{0} & \mathbf{0} & \mathbf{0} \\ \mathbf{0} & -\mathbf{I} & \mathbf{0} & \mathbf{0} \\ \mathbf{0} & \mathbf{0} & \mathbf{I} & \mathbf{0} \\ \mathbf{0} & \mathbf{0} & \mathbf{0} & -\mathbf{I} \end{bmatrix} l_{\mathbf{T}}^x, \tag{6}$$

$\bar{\mathbf{T}} : \mathbb{R}^{24} \to \mathbb{R}^{12\times 12}$ and $\mathbf{H}_{\mathbf{T}} : \mathbb{R}^{12} \to \mathbb{R}^{12\times 24}$ are linear maps that are derived in Appendix A. Thus, we have transformed the complex model (2) into a real model (5) that is linear with respect to the parameter vector $\theta^{\mathbf{T}}$.

Remark. Although line model (5) assumes a 24-dimensional unknown parameter vector $\theta^{\mathbf{T}}$, in most practical estimation scenarios, more structural information regarding the parameter vector is available a-priori. For example, the real part and the non-diagonal entries of the shunt admittance matrix $\mathbf{Y}_l$ have negligible values for short lines. If such additional information is available, then the dimension of the parameter vector $\theta^{\mathbf{T}}$ can be reduced. This reduction generally leads to more accurate estimates of the remaining unknown parameters. It is easy to see that formulation (5) can be generalized to any dimension $\mathcal{S}_\theta$ of the parameter vector $\theta^{\mathbf{T}}$ and the linear maps $\bar{\mathbf{T}}$ and $\mathbf{H}_{\mathbf{T}}$ can be recomputed according to the new dimension by repeating the method discussed in Appendix A.

B. Impedance and Admittance Matrix Models

There are two other line models that are typically used in the literature to link the phasors with the line parameters.

(1) *The Y-line model*: The admittance matrix can be used to express the relationship between the voltage phasors $v = [(v^r)', (v^s)']'$ and the current phasors $i = [(i^r)', (i^s)']'$ as follows:

$$i = \begin{bmatrix} {\mathbf{Z}_l}^{-1} + \frac{\mathbf{Y}_l}{2} & -{\mathbf{Z}_l}^{-1} \\ -{\mathbf{Z}_l}^{-1} & {\mathbf{Z}_l}^{-1} + \frac{\mathbf{Y}_l}{2} \end{bmatrix} v \tag{7}$$

(2) *The Z-line model*: The same relation (7) can be rewritten using the impedance matrix as follows:

$$v = \begin{bmatrix} \frac{\mathbf{Z}_l}{2} + {\mathbf{Y}_l}^{-1} & {\mathbf{Y}_l}^{-1} \\ {\mathbf{Y}_l}^{-1} & \frac{\mathbf{Z}_l}{2} + {\mathbf{Y}_l}^{-1} \end{bmatrix} i \tag{8}$$

Clearly the Y-line model and the Z-line model are not linear if expressed in terms of the parameter vector $\theta^{\mathbf{T}}$ due to the presence of the inverse terms $\mathbf{Z}_l^{-1}$ and $\mathbf{Y}_l^{-1}$. Thus, we introduce parameter vectors $\theta^{\mathbf{Y}} \in \mathbb{R}^{24}$ and $\theta^{\mathbf{Z}} \in \mathbb{R}^{24}$ to parameterize the Y-line model and the Z-line model, respectively. We define $\theta^{\mathbf{Y}}$ such that it differs from $\theta^{\mathbf{T}}$ only in components 4 through 15 for which we define

$$\mathbf{Z}_l^{-1} = \begin{bmatrix} \theta_4^{\mathbf{Y}} \theta_6^{\mathbf{Y}} \theta_8^{\mathbf{Y}} \\ \theta_6^{\mathbf{Y}} \theta_{10}^{\mathbf{Y}} \theta_{12}^{\mathbf{Y}} \\ \theta_8^{\mathbf{Y}} \theta_{12}^{\mathbf{Y}} \theta_{14}^{\mathbf{Y}} \end{bmatrix} + j \begin{bmatrix} \theta_5^{\mathbf{Y}} \theta_7^{\mathbf{Y}} \theta_9^{\mathbf{Y}} \\ \theta_7^{\mathbf{Y}} \theta_{11}^{\mathbf{Y}} \theta_{13}^{\mathbf{Y}} \\ \theta_9^{\mathbf{Y}} \theta_{13}^{\mathbf{Y}} \theta_{15}^{\mathbf{Y}} \end{bmatrix} \tag{9}$$

The parameter vector $\theta^{\mathbf{Z}}$ is also defined similarly.

Similar to (5), (7) and (8) can be rewritten as follows:

$$l_{\mathbf{Y}}^s = \bar{\mathbf{Y}}(\theta^{\mathbf{Y}}) l_{\mathbf{Y}}^r = \mathbf{H}_{\mathbf{Y}}(l_{\mathbf{Y}}^r)\theta^{\mathbf{Y}} + \gamma_{\mathbf{Y}}(l_{\mathbf{Y}}^r), \tag{10}$$

$$l_{\mathbf{Z}}^s = \bar{\mathbf{Z}}(\theta^{\mathbf{Z}}) l_{\mathbf{Z}}^r = \mathbf{H}_{\mathbf{Z}}(l_{\mathbf{Z}}^r)\theta^{\mathbf{Z}} + \gamma_{\mathbf{Z}}(l_{\mathbf{Z}}^r), \tag{11}$$

where $\gamma_{\mathbf{Y}}(l_{\mathbf{Y}}^r) = \gamma_{\mathbf{Z}}(l_{\mathbf{Z}}^r) = 0$, $l_{\mathbf{Y}}^s = l_{\mathbf{Z}}^r = [\mathcal{R}(i^r)', \mathcal{R}(i^s)', \mathcal{I}(i^r)', \mathcal{I}(i^s)']'$, $l_{\mathbf{Y}}^r = l_{\mathbf{Z}}^s = [\mathcal{R}(v^r)', \mathcal{R}(v^s)', \mathcal{I}(v^r)', \mathcal{I}(v^s)']'$, and $\mathbf{H}_{\mathbf{Y}}, \bar{\mathbf{Y}}, \bar{\mathbf{Z}}, \mathbf{H}_{\mathbf{Z}}$ are linear maps that can be computed using a method similar to the one described in Appendix A.

C. Noise Model

The noise in the measurements are introduced at two sources: (1) at the instrument transformers (ITs), i.e., the voltage transformers for voltage measurements and the current transformers for current measurements, (2) at the PMUs. Hence, the total noise is the sum of the noises at the ITs and the PMUs. To statistically characterize the noise introduced by a measuring device, we make use of the standard specifications of the device.

The manufacturers of instrument transformers specify the maximum errors - as percentages (α) in case of magnitudes and as absolute values (β) in case of phases - introduced by such devices. The values of α and β for different classes of instrument transformers are given in Table I [29]. For, PMUs the maximum errors are specified similarly. In this paper, we consider class 0.1 PMUs that are characterized by $\alpha = 0.1\%$ and $\beta = 10^{-4}$ (e.g. [30]). Note that the maximum errors are the same for voltage and current transformers.

We assume that the measurement noise is Gaussian, unbiased, and that it lies within the specified maximum bound with probability 0.9973. Hence, to find the standard deviation, we divide the value of the maximum error by 3. More specifically, let ρ and ϕ, respectively, denote the magnitude and phase of a complex phasor w, i.e., $w = \rho e^{j\phi}$. Then the noise Δ_ρ and Δ_ϕ on ρ and ϕ are assumed to be distributed as $\Delta_\rho \sim \mathcal{N}(0, \frac{\alpha\rho}{3})$, and $\Delta_\phi \sim \mathcal{N}(0, \beta/3)$, respectively, where α and β are as defined before (see Table I for values).

TABLE I
MAXIMUM ERRORS FOR DIFFERENT CLASSES OF INSTRUMENT TRANSFORMERS

Transformer Class	Max. magnitude error (α) [%]	Max. phase error (β) [rad]
0.1	0.1	1.5×10^{-3}
0.2	0.2	3×10^{-3}
0.5	0.5	9×10^{-3}
1	1	18×10^{-3}

The noise is Gaussian in polar coordinates, whereas we use rectangular coordinates in our estimation procedures. The noise transformation from polar to rectangular coordinates is non-linear and hence it does not preserve Gaussianity of the noise. However, for the parameters of Table I, we observe numerically that the distribution of the noise transformed in the rectangular coordinates is very close to the Gaussian distribution. This is shown by the quantile-quantile (QQ) plots in Figures 2 and 3 for Class 1 ITs, which have the highest error among all classes of ITs. We observe that the quantiles of the transformed noise (scaled by its standard deviation) match very closely with those of a standard normal random variable. For this reason, we treat the noise in the rectangular coordinates as Gaussian random variables.

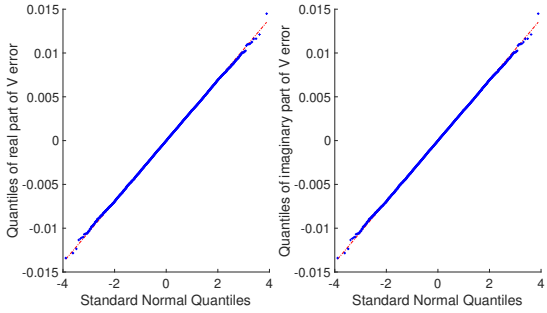

Fig. 2. QQ plots for noise on voltages measured by a Class 1 IT

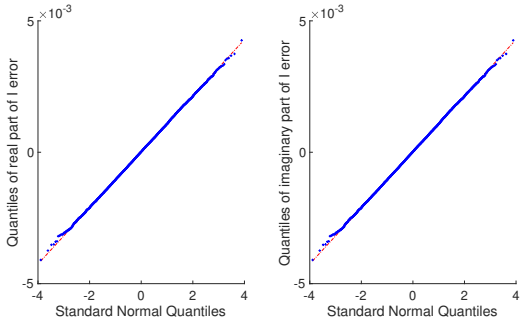

Fig. 3. QQ plots for noise on currents measured by a Class 1 IT.

To find the mean and covariances of the transformed noise, we first denote the noisy measurement of the phasor $w = \rho e^{j\phi}$ as $\tilde{w} = \tilde{\rho} e^{j\tilde{\phi}}$. If Δ_{re} and Δ_{im}, respectively, denote the noise in the real and imaginary parts, then it can be shown using moment generating functions [31] that

$$\Delta_{re} = \tilde{\rho}\cos(\tilde{\phi}) - \rho\cos(\phi) \tag{12}$$

$$E[\Delta_{re}] = \left(e^{-\frac{1}{2}\sigma_\phi^2} - 1\right)\cos(\phi)\rho \tag{13}$$

$$E[\Delta_{re}^2] = \frac{1}{2}(1+\frac{\alpha^2}{9})\rho^2(1+e^{-2\sigma_\phi^2}\cos(2\phi)) + \rho^2\cos^2(\phi)(1-2e^{(-\frac{1}{2}\sigma_\phi^2)}) \tag{14}$$

$$\Delta_{im} = \tilde{\rho}\sin(\tilde{\phi}) - \rho\sin(\phi) \tag{15}$$

$$E[\Delta_{im}] = \left(e^{-\frac{1}{2}\sigma_\phi^2} - 1\right)\sin(\phi)\rho \tag{16}$$

$$E[\Delta_{im}^2] = \frac{1}{2}\left(1+\frac{\alpha^2}{9}\right)\rho^2\left(1+e^{-2\sigma_\phi^2}\cos(2\phi)\right) + \rho^2\sin^2(\phi)\left(1-2e^{-\frac{1}{2}\sigma_\phi^2}\right) \tag{17}$$

$$E[\Delta_{re}\Delta_{im}] = \frac{1}{2}\sin(2\phi)\left[\left(1+\frac{\alpha^2}{9}\right)\rho^2 e^{-2\sigma_\phi^2} - 2\rho^2 e^{\left(-\frac{1}{2}\sigma_\phi^2\right)} + \rho^2\right], \tag{18}$$

where $E[\cdot]$ is the expectation operator and $\sigma_\phi = \beta/3$. We note from (13) and (16) that the noise in the rectangular coordinates is biased in general. However, for the parameters of Table I, we observe that the bias is negligible. We further observe that, for the parameters of interest, the correlation between the real and imaginary parts of the noise is not negligible, as is routinely assumed in the existing literature.

We note from (13)-(18) that covariances of noise in rectangular coordinates depend on the true value of the measurements that are unknown in practice. In our estimation procedures, these covariances are computed by replacing the true values by the measured values. We have numerically observed that doing so has a negligible effect on the estimation procedures proposed in this paper.

Remark. We have assumed that measurement noise in polar coordinates is normally distributed, which is standard in the literature [30], [21], [23]. Even if this assumption is only approximately true, numerical simulations show that, for the parameter values shown in Table I, the noise in the rectangular coordinates is very close to Gaussian noise with covariances given by (13)-(18).

D. Generalized Statistical Model

Here, we present a general statistical model that incorporates the line models and the noise model discussed thus far.

Let $(x_i, y_i) \in \mathbb{R}^{12}\times\mathbb{R}^{12}$ and $(\tilde{x}_i, \tilde{y}_i) \in \mathbb{R}^{12}\times\mathbb{R}^{12}$ denote the true and measured pairs of i^{th} phasors with separated real and imaginary parts, respectively. Furthermore, let $\theta \in \mathbb{R}^{\mathcal{S}_\theta}$ be the unknown parameter vector of dimension $\mathcal{S}_\theta$ to be estimated. Then the generalized model is given by

$$y_i = \bar{\mathbf{B}}(\theta)x_i = \mathbf{H}(x_i)\theta + \gamma(x_i), \tag{19}$$

$$\tilde{y}_i = y_i + \Delta_{y_i}, \quad \Delta_{y_i} \sim \mathcal{N}(0, \mathbf{Q}_{y_i}), \tag{20}$$

$$\tilde{x}_i = x_i + \Delta_{x_i}, \quad \Delta_{x_i} \sim \mathcal{N}(0, \mathbf{Q}_{x_i}), \tag{21}$$

where the mapping between the different notations of the general model to the previously discussed line models is given in Table II, $\Delta_{y_i}, \Delta_{x_i} \in \mathbb{R}^{12}$ denote the noise on y_i and x_i, respectively; and $\mathbf{Q}_{y_i}, \mathbf{Q}_{x_i} \in \mathbb{R}^{12\times 12}$ denote the noise covariance matrices of $\Delta_{y_i}, \Delta_{x_i}$, respectively. The entries of the covariance matrices $\mathbf{Q}_{y_i}$ and $\mathbf{Q}_{x_i}$ can be computed using the parameters of Table I and transformation equations (14), (17) and (18).

If we have N measurements of the phasors, then combining all the measurements gives us the following more compact representation of the model:

$$y = \bar{\mathbf{B}}_N(\theta)x = \mathbf{H}_N(x)\theta + \gamma(x) \tag{22}$$

$$\tilde{y} = y + \Delta_y \quad \Delta_y \sim \mathcal{N}(0, \mathbf{Q}_y) \tag{23}$$

$$\tilde{x} = x + \Delta_x \quad \Delta_x \sim \mathcal{N}(0, \mathbf{Q}_x) \tag{24}$$

where $x = [x_1', \ldots, x_N']', y = [y_1', \ldots, y_N']' \in \mathbb{R}^{12N}$, $\mathbf{H}_N(x) = [\mathbf{H}(x_1)', \ldots, \mathbf{H}(x_N)']' \in \mathbb{R}^{12N\times \mathcal{S}_\theta}$, $\gamma_N(x) = [\gamma(x_1)', \ldots, \gamma(x_N)']' \in \mathbb{R}^{12N}$, $\mathbf{Q}_x = \mathsf{diag}(\mathbf{Q}_{x_1}, \ldots, \mathbf{Q}_{x_N})$, $\mathbf{Q}_y = \mathsf{diag}(\mathbf{Q}_{y_1}, \ldots, \mathbf{Q}_{y_N}) \in \mathbb{R}^{12N\times 12N}$, $\bar{\mathbf{B}}_N(\theta) = \mathsf{diag}(\bar{\mathbf{B}}(\theta), \ldots, \bar{\mathbf{B}}(\theta)) \in \mathbb{R}^{12N\times 12N}$.

TABLE II
MAPPING OF NOTATIONS BETWEEN THE GENERAL STATISTICAL MODEL AND DIFFERENT LINE MODELS

Stat. Model	T-line model	Z-line model	Y-line model
y_i	$l^s_{\mathbf{T}}(i)$	$l^s_{\mathbf{Z}}(i)$	$l^s_{\mathbf{Y}}(i)$
x_i	$l^r_{\mathbf{T}}(i)$	$l^r_{\mathbf{Z}}(i)$	$l^r_{\mathbf{Y}}(i)$
$\bar{\mathbf{B}}$	$\bar{\mathbf{T}}$	$\bar{\mathbf{Z}}$	$\bar{\mathbf{Y}}$
$\gamma(\cdot)$	$\gamma_{\mathbf{T}}(\cdot)$	$\gamma_{\mathbf{Z}}(\cdot)$	$\gamma_{\mathbf{Y}}(\cdot)$
θ	$\theta^{\mathbf{T}}$	$\theta^{\mathbf{Z}}$	$\theta^{\mathbf{Y}}$
$\mathbf{H}$	$\mathbf{H}_{\mathbf{T}}$	$\mathbf{H}_{\mathbf{Z}}$	$\mathbf{H}_{\mathbf{Y}}$

III. Proposed Estimation Methods

We now describe different estimation methods that use the statistical model defined in the previous section. The objective is to estimate the parameter vector θ from the noisy measurement vectors $\tilde{x}$ and $\tilde{y}$.

A. Maximum-Likelihood Estimator - Weighted Total Least-Squares

The maximum-likelihood estimator, also referred to as the weighted total least-squares (WTLS), uses the true statistical model defined above to compute an estimator of θ. Clearly, from (22)-(24), this estimator can be found by solving the following minimization problem:

$$\min_\theta \min_x (\tilde{x} - x)^T \mathbf{Q}_x^{-1} (\tilde{x} - x) + \left(\tilde{y} - \bar{\mathbf{B}}_N(\theta)x\right)^T \mathbf{Q}_y^{-1} \left(\tilde{y} - \bar{\mathbf{B}}_N(\theta)x\right) \tag{25}$$

Note that the inner minimization problem in x is convex and can be solved in closed form as a function of θ. The solution $\hat{x}(\theta)$ is given as

$$\hat{x}(\theta) = \left(\mathbf{Q}_x^{-1} + \bar{\mathbf{B}}_N^T(\theta)\mathbf{Q}_x^{-1}\bar{\mathbf{B}}_N(\theta)\right)^{-1} \times \left(\mathbf{Q}_x^{-1}\tilde{x} + \bar{\mathbf{B}}_N^T(\theta)\mathbf{Q}_y^{-1}\tilde{y}\right), \tag{26}$$

Finally, to obtain θ, we solve the following problem:

$$\hat{\theta}_{ml} = \arg\min_\theta (\tilde{x} - \hat{x}(\theta))^T \mathbf{Q}_x^{-1} (\tilde{x} - \hat{x}(\theta)) + (\tilde{y} - \mathbf{H}_N(\hat{x}(\theta))\theta - \gamma_N(\hat{x}(\theta)))^T \mathbf{Q}_y^{-1} \times (\tilde{y} - \mathbf{H}_N(\hat{x}(\theta))\theta - \gamma_N(\hat{x}(\theta))).$$

We note that the above optimization problem is non-convex. Therefore, only local optimal solutions can be found using numerical solvers.

B. Ordinary Total Least-Squares

The ordinary total least-squares (OTLS) method is typically used in error-in-variables regression [32], [33]. Here, the objective is to estimate a parameter matrix $\mathbf{U} \in \mathbb{C}^{p\times q}$, which satisfies the linear relationship

$$\mathbf{C}\mathbf{U} = \mathbf{D} \tag{27}$$

with $\mathbf{C} \in \mathbb{C}^{n\times p}$ and $\mathbf{D} \in \mathbb{C}^{n\times q}$ from noisy observations $\tilde{\mathbf{C}}$ of $\mathbf{C}$ and $\tilde{\mathbf{D}}$ of $\mathbf{D}$. Note that in ordinary least-squares regression, errors are assumed to be present only in the matrix $\mathbf{D}$. In the special case where $\mathbf{D}$ and $\mathbf{U}$ are vectors ($q = 1$), we denote them by lower cases d and u.

In general, (27) can be rewritten in the following form

$$\begin{bmatrix}\mathbf{C}\ \mathbf{D}\end{bmatrix}\begin{bmatrix}\mathbf{U}\\ -\mathbf{I}_{q\times q}\end{bmatrix} = \mathbf{0}_{n\times q}. \tag{28}$$

The above can be used to find denoised $\hat{\mathbf{C}}$ and $\hat{\mathbf{D}}$ as follows:

$$\hat{\mathbf{C}}, \hat{\mathbf{D}} = \arg\min_{\mathbf{C},\mathbf{D}} \left\| \begin{bmatrix}\mathbf{C}\ \mathbf{D}\end{bmatrix} - \begin{bmatrix}\tilde{\mathbf{C}}\ \tilde{\mathbf{D}}\end{bmatrix} \right\|_F \tag{29}$$

$$\text{subject to} \quad \mathsf{rank}\left(\begin{bmatrix}\mathbf{C}\ \mathbf{D}\end{bmatrix}\right) \le q. \tag{30}$$

Note that the rank constraint in the above optimization is equivalent to the existence of a parameter matrix $\mathbf{U} \in \mathbb{R}^{p\times q}$ satisfying (28). The above optimization is an instance of the low-rank approximation problem for the observed data matrix $[\tilde{\mathbf{C}}\ \ \tilde{\mathbf{D}}]$ and can be solved using the singular value decomposition (SVD) of $[\tilde{\mathbf{C}}\ \ \tilde{\mathbf{D}}]$. Let the SVD of $[\tilde{\mathbf{C}}\ \ \tilde{\mathbf{D}}]$ be

$$[\tilde{\mathbf{C}}\ \ \tilde{\mathbf{D}}] = \begin{bmatrix}\mathbf{U}_C\ \mathbf{U}_D\end{bmatrix}\begin{bmatrix}\mathbf{\Sigma}_C & \mathbf{0}_{p\times q}\\ \mathbf{0}_{q\times p} & \mathbf{\Sigma}_D\end{bmatrix}\begin{bmatrix}\mathbf{V}_{C,C} & \mathbf{V}_{C,D}\\ \mathbf{V}_{D,C} & \mathbf{V}_{D,D}\end{bmatrix}^*$$

where $\mathbf{A}^*$ denotes the matrix conjugate of $\mathbf{A} \in \mathbb{C}^{n\times n}$.

Then the parameter matrix $\mathbf{U}$ is estimated as (see [32]):

$$\hat{\mathbf{U}}_{\text{tls}} = -\mathbf{V}_{C,D}\mathbf{V}_{D,D}^{-1}. \tag{31}$$

We note that $\hat{\mathbf{C}}, \hat{\mathbf{D}}$ are the maximum-likelihood estimates of $\mathbf{C}, \mathbf{D}$ only when the noise $[\Delta_{\mathbf{C}}\ \ \Delta_{\mathbf{D}}]$ on the data matrix $[\mathbf{C}\ \ \mathbf{D}]$ has independent and identically distributed (zero-mean Gaussian) rows, which is an approximation of the true statistical model.

1) Structured OTLS: The structured OTLS (SOTLS) problem is obtained by replacing

$$\mathbf{C} = \mathbf{H}_N(x), \quad u = \theta, \quad d = y - \gamma_N(x), \tag{32}$$

The estimate $\hat{\theta}_{tls}$ of θ can therefore be obtained using (31).

2) Unstructured OTLS: The unstructured OTLS (UOTLS) problem in the context of the estimation problem of $\bar{\mathbf{B}}$ is solved by putting

$$\mathbf{C} = \begin{bmatrix} x_1' \\ \vdots \\ x_N' \end{bmatrix}, \quad \mathbf{U} = \bar{\mathbf{B}}(\theta)', \quad \mathbf{D} = \begin{bmatrix} y_1' \\ \vdots \\ y_N' \end{bmatrix}, \tag{33}$$

C. Weighted and Ordinary Least-Squares (WLS and OLS)

In the method of ordinary or weighted least-squares, the noise on the right-hand side of (22) is ignored, i.e., it is assumed that $\tilde{x} = x$. In this case, the well known least-squares estimation formula for weighted least-squares (WLS) yields the following estimate of θ:

$$\hat{\theta}_{wls} = \left(\mathbf{H}_N(\tilde{x})'\mathbf{Q}_y^{-1}\mathbf{H}_N(\tilde{x})\right)^{-1}\mathbf{H}_N(\tilde{x})'\mathbf{Q}_y^{-1}(\tilde{y} - \gamma_N(x)), \tag{34}$$

The ordinary least-squares (OLS) estimate of θ is obtained by replacing $\mathbf{Q_y}$ in the above by the identity matrix.

1) Enhanced WLS (EWLS): Note that in the WLS for the T-line model the roles of the vectors y and x can be interchanged since we have

$$l^s = \bar{\mathbf{T}}(\theta^{\mathbf{T}})l^r \quad \text{and} \quad l^r = \bar{\mathbf{T}}(\theta^{\mathbf{T}})l^s.$$

under the approximation that $\mathbf{Y}_l\mathbf{Z}_l \approx 0$. In EWLS, we first estimate $\theta^{\mathbf{T}}$ by using the WLS method described above. Then we switch the roles of x and y in (34) from $l^r_{\mathbf{T}}$ and $l^s_{\mathbf{T}}$ to $l^s_{\mathbf{T}}$ and $l^r_{\mathbf{T}}$, respectively, and re-estimate $\theta^{\mathbf{T}}$. We then take the average of the two estimates.

IV. Simulations

We now evaluate the performance of the proposed estimation methods by using a dataset containing PMU measurements of voltage and current phasors of a 125kV sub-transmission grid installed in Lausanne. The grid has 7 buses that are connected by 10 lines as shown in Figure 4. All the lines are short and have length less than 5km. The true values of the line parameters are given in the dataset and are shown in Table III (in per unit (p.u.)) for two different lines (lines numbered 2 and 10 in Figure 4) of which one is coaxial (line 2) and the other is non-coaxial (line 10). We used 72.2 kV as the base value for voltage and 10 MW as the base value of power to obtain the values in per unit.

The dataset contains one day of PMU measurements of current and voltage phasors at both ends of each line at a frequency of 50 measurements per second. This results in a maximum of $N = 24 \times 3600 \times 50 \approx 4.3 \times 10^6$ samples for each line. To reliably evaluate the performance of different estimation methods, we follow the procedure described below

TABLE III
True parameter values of lines 2 and 10 in p.u.

Parameter	Values $\times 10^{-4}$ p.u.	
	Non-Coaxial	Coaxial
$(\mathbf{Z}_l)_{11} = (\mathbf{Z}_l)_{22} = (\mathbf{Z}_l)_{33}$	$18 + j51$	$2.8 + j5.2$
$(\mathbf{Z}_l)_{12} = (\mathbf{Z}_l)_{13} = (\mathbf{Z}_l)_{23}$	$6.3 + j21.0$	$1.2 - j1.2$
$(\mathbf{Y}_l)_{11} = (\mathbf{Y}_l)_{22} = (\mathbf{Y}_l)_{33}$	$j50$	$j530$
$(\mathbf{Y}_l)_{12} = (\mathbf{Y}_l)_{13} = (\mathbf{Y}_l)_{23}$	$-j6.6$	0

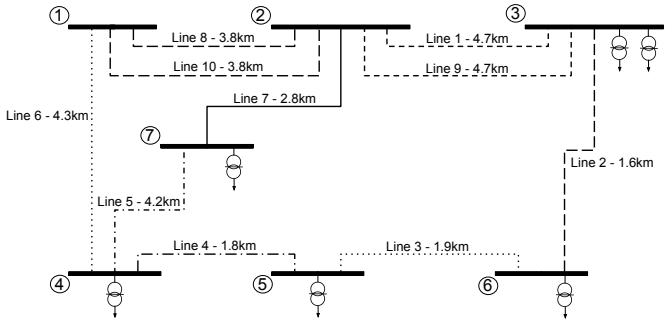

Fig. 4. 125kV sub-transmission grid at Lausanne, Switzerland.

to generate the voltage and current phasors for one end of each line:

Step 1: We take the measurements from one end of the line from the dataset. We treat them as the true phasor values.

Step 2: We generate the true phasor values at the other-end of the line using the phasors of Step 1, the line parameters of Table III, and equation (1).

Step 3: We add noise to the phasors in Step 1 and Step 2.

The detailed procedure for data generation is described as Algorithm 1 below. Note that this procedure retains the effect of different loading conditions present in the original data.

Using the samples generated by the above procedure and different estimation methods, we estimate the line parameters. The metrics used to evaluate the performance of an estimator $\hat{\theta}$ of the true parameter vector θ are the average relative error, the average relative error per component, and the mean squared error (MSE) defined as follows

$$e_\theta = \frac{1}{\mathcal{S}_\theta}\sum_{i=1}^{\mathcal{S}_\theta}\left|\frac{\theta_i - \hat{\theta}_i}{\theta_i}\right| \times 100, \tag{35}$$

$$e_{\theta_i} = \left|\frac{\theta_i - \hat{\theta}_i}{\theta_i}\right| \times 100 \quad \forall i \in [1, \mathcal{S}_\theta], \tag{36}$$

$$MSE(\theta) = \frac{1}{\mathcal{S}_\theta}\sum_{i=1}^{\mathcal{S}_\theta}(\theta_i - \hat{\theta}_i)^2 \tag{37}$$

The results are obtained by repeating our experiments 10 times (with different realizations of noise) and then averaging the results. To simplify our notations, in the following, we use θ without a superscript to denote the parameter vector $\theta^{\mathbf{T}}$ of the T-line model, unless specified otherwise.

Remark. From Table III, we observe that $\mathcal{R}(\mathbf{Y}_l) = \mathbf{0}$ for both lines. This is because these lines are short (< 5 km) and

Algorithm 1 Data generation

procedure GENDATA
  for each line **do**
    Construct $\mathbf{Z}_l, \mathbf{Y}_l$ from Table III
    for $n = 1 : N$ **do**
      Obtain v_n^r, i_n^r from the dataset
      $$\begin{bmatrix} v_n^s \\ i_n^s \end{bmatrix} \leftarrow \begin{bmatrix} \mathbf{I} + \frac{\mathbf{Z}_l\mathbf{Y}_l}{2} & -\mathbf{Z}_l \\ \mathbf{Y}_l\left(\mathbf{I} + \frac{\mathbf{Z}_l\mathbf{Y}_l}{4}\right) - \left(\mathbf{I} + \frac{\mathbf{Z}_l\mathbf{Y}_l}{2}\right) & \end{bmatrix} \begin{bmatrix} v_n^r \\ i_n^r \end{bmatrix}$$
      for $x = [v_n^r, v_n^s, i_n^r, i_n^s]$ **do**
        $\Delta_\rho \leftarrow \mathcal{N}(0, \frac{\alpha}{3}|x|)$
        $|x| \leftarrow |x| + \Delta_\rho$
        $\Delta_\phi \leftarrow \mathcal{N}(0, \frac{\beta}{3})$
        $\arg(x) \leftarrow \arg(x) + \Delta_\phi$
        $x = |x|\, e^{j \arg(x)}$
      end for
    end for
  end for
end procedure

for short lines the resistive parts of the shunt elements have negligible values. We use this side information to reduce the size of the parameter vector θ from $\mathcal{S}_\theta = 24$ to $\mathcal{S}_\theta = 18$ by eliminating the last six components. Furthermore, for the coaxial line, we have $\mathcal{I}((\mathbf{Y}_l)_{ij}) = 0$ for $j \neq i$, which leads to a further reduction of the dimension of the parameter vector of this line to $\mathcal{S}_\theta = 15$. We further note that the diagonal and non-diagonal entries of $\mathbf{Z}_l$ (and $\mathbf{Y}_l$) are equal. If we use this information then the dimension of the parameter space reduces to $\mathcal{S}_\theta = 5$ for the coaxial line and $\mathcal{S}_\theta = 6$ for the non-coaxial line. However, we can only use this information when it is known that the lines are fully transposed. We test our estimation procedures both with and without this assumption. The parameters of the lines under different line models is given in Table IV and Table V using smaller parameter spaces and the corresponding parameterization of different line models are given in Appendix B.

TABLE IV
TRUE VALUE OF THE PARAMETERS OF COAXIAL LINE ($\mathcal{S}_\theta = 5$)

$\theta_1^{\mathbf{T}}$	2.8×10^{-4}	$\theta_1^{\mathbf{Y}}$	7.3×10^{2}	$\theta_1^{\mathbf{Z}}$	2.8×10^{-4}
$\theta_2^{\mathbf{T}}$	5.2×10^{-4}	$\theta_2^{\mathbf{Y}}$	3.7×10^{2}	$\theta_2^{\mathbf{Z}}$	5.2×10^{-4}
$\theta_3^{\mathbf{T}}$	1.2×10^{-4}	$\theta_3^{\mathbf{Y}}$	-1.3×10^{3}	$\theta_3^{\mathbf{Z}}$	1.2×10^{-4}
$\theta_4^{\mathbf{T}}$	-1.2×10^{-4}	$\theta_4^{\mathbf{Y}}$	2.2×10^{2}	$\theta_4^{\mathbf{Z}}$	-1.2×10^{-4}
$\theta_5^{\mathbf{T}}$	5.3×10^{-2}	$\theta_5^{\mathbf{Y}}$	5.3×10^{-2}	$\theta_5^{\mathbf{Z}}$	1.9×10^{1}

A. Comparison of Different Line Models

We first compare different line models in terms of their noise sensitivities. Noise sensitivity can be measured by the Fisher Information Matrix (FIM), that quantifies the information that measurements carry about an unknown parameter vector. According to the Cramer-Rao theorem, the trace of the inverse of the FIM gives a lower bound on the MSE of any unbiased estimator. Hence, a way of comparing different line models is to compare their corresponding Cramer-Rao bounds (CRBs) that give the lowest achievable MSEs (by an unbiased estimator) for different line models.

TABLE V
TRUE VALUE OF THE PARAMETERS OF OVERHEAD LINE ($\mathcal{S}_\theta = 6$)

$\theta_1^{\mathbf{T}}$	1.8×10^{-3}	$\theta_1^{\mathbf{Y}}$	86	$\theta_1^{\mathbf{Z}}$	1.8×10^{-3}
$\theta_{2^{\mathbf{T}}}$	5.1×10^{-3}	$\theta_2^{\mathbf{Y}}$	-27	$\theta_2^{\mathbf{Z}}$	5.1×10^{-3}
$\theta_3^{\mathbf{T}}$	6.3×10^{-4}	$\theta_3^{\mathbf{Y}}$	-2.3×10^{2}	$\theta_3^{\mathbf{Z}}$	6.3×10^{-4}
$\theta_4^{\mathbf{T}}$	2.1×10^{-3}	$\theta_4^{\mathbf{Y}}$	64	$\theta_4^{\mathbf{Z}}$	2.1×10^{-3}
$\theta_5^{\mathbf{T}}$	5.0×10^{-3}	$\theta_5^{\mathbf{Y}}$	5.0×10^{-3}	$\theta_5^{\mathbf{Z}}$	2.1×10^{2}
$\theta_6^{\mathbf{T}}$	-6.6×10^{-4}	$\theta_6^{\mathbf{Y}}$	-6.6×10^{-4}	$\theta_6^{\mathbf{Z}}$	3.2×10^{1}

Using the log-likelihood function in (25), we derive the FIM for the general statistical model, described by (22)-(24). The FIM is given by

$$\mathcal{I}(x,\theta) = \begin{bmatrix} \mathbf{Q}_x^{-1} + \bar{\mathbf{B}}_N(\theta)\mathbf{Q}_y^{-1}\bar{\mathbf{B}}_N(\theta)' & \bar{\mathbf{B}}_N(\theta)\mathbf{Q}_y^{-1}\mathbf{H}_N(x) \\ \mathbf{H}_N(x)'\mathbf{Q}_y^{-1}\bar{\mathbf{B}}_N(\theta)' & \mathbf{H}_N(x)'\mathbf{Q}_y^{-1}\mathbf{H}_N(x)' \end{bmatrix}$$

In Table VI, we compare the CRBs of different line models for two extreme classes of ITs assuming $\mathcal{S}_\theta = 18$ and $N = 1000$. It is clear from the comparison, that the T-line model has the lowest MSE achievable by any unbiased estimator.

TABLE VI
COMPARISON BETWEEN T-LINE MODEL, Y-LINE MODEL AND Y-LINE MODEL IN TERMS OF CRB FOR $\mathcal{S}_\theta = 18$ AND $N = 1000$

T-line model		Z-line model		Y-line model	
0.1 IT	1 IT	0.1 IT	1 IT	0.1 IT	1 IT
2.0×10^{-4}	0.022	8.2×10^5	9.2×10^7	8500	9.6×10^5

As the MSE is an absolute measure of error, we now present a comparison of the line models based on the relative errors. Using the WLS method, we estimate the parameters of the non-coaxial line for each line model and for two extreme classes of ITs. From Table III and Table V, we note that although we have an 18-dimensional parameter space, we are actually measuring 6 different parameters. Hence, to compactly represent our results, we take the average of those components of the (18 dimensional) parameter vector which measure the same quantity. Finally, to have a fair comparison we report all the errors in the parameter space of the Y-line model. This is done in Table VII, from where it is clear that the relative errors are the least when T-line model is used.

To study the effect of variation of the length of the line on the quality of estimates produced by the three line models we scale the parameters by different line lengths and repeat our experiments. In Figure 5, we plot the relative error (measured by the 2-norm) in estimating the matrix $\bar{\mathbf{Y}}(\theta^{\mathbf{Y}})$ as a function of the length of the line. It is clear that for short lines (with length less than 80km) the T-line model results in the least relative error; whereas for longer lines, either the Z-line model (for line lengths between 80km and 180km) or the Y-line model (for line lengths above 180km) produces the

TABLE VII
COMPARISON BETWEEN T, Z AND Y LINE MODELS WITH $\mathcal{S}_\theta = 18$ AND $N = 3 \times 10^6$

Relative errors	T-line model		Z-line model		Y-line model	
	0.1 IT	1 IT	0.1 IT	1 IT	0.1 IT	1 IT
$e_{\theta_1^{\mathbf{Y}}}$	4.0	7.2	34	150	80	99
$e_{\theta_2^{\mathbf{Y}}}$	14	21	36	320	67	99
$e_{\theta_3^{\mathbf{Y}}}$	1.8	2.8	12	97	80	99
$e_{\theta_4^{\mathbf{Y}}}$	5.5	7.7	43	120	69	99
$e_{\theta_5^{\mathbf{Y}}}$	24	25	1800	400	460	130
$e_{\theta_6^{\mathbf{Y}}}$	180	190	13000	3100	2900	160

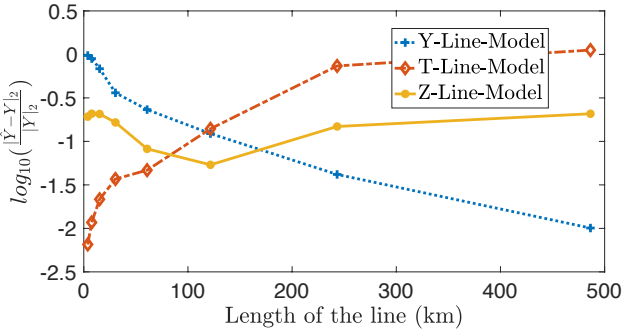

Fig. 5. Evolution of estimation error with the length of the line for different line models.

most accurate estimates. The accuracy of the T-line model deteriorates with the increase in the line length because the accuracy of the 'short-line approximation' reduces as the line length increases. However, in this case, the accuracy of the Y-line model improves since the effect of noise on the line parameters reduces.

There are several reasons for the T-line model to be the most accurate one in estimating parameters for short lines. One prominent factor is that the line parameters have similar order of magnitude under the T-line model, whereas they are very different under other line models. This is evident from the true values listed in Tables IV and Table V. Another reason is that in the T-line model the estimation of $\mathbf{Y}_l$ and $\mathbf{Z}_l$ can be done independently of each other as is evident from (2). This is not true in the other models.

B. Comparison among Different Estimation Methods

In this subsection, we compare different estimation methods in terms of computing time and accuracy. We choose the T-line model for all experiments since this provides the best accuracy among all the line models.

In Table VIII, we compare the MSEs of OLS, UOTLS, and SOTLS for both lines and for $N = 3 \times 10^6$. It can be observed form the table that the OLS significantly outperforms the UOTLS and SOTLS methods. In fact the SOTLS and UOTLS completely fail at recovering the parameters in the presence of noise. This is mainly due to the fact that both methods assume the measurement noise to be homoscedastic (with diagonal covariance matrix), which is not true for the generated samples.

TABLE VIII
MSE'S FOR OLS, UOTLS, AND SOTLS WITH IT OF CLASS 1 AND $N = 3 \times 10^6$

	Coaxial line ($\mathcal{S}_\theta = 15$)	Non-coaxial line ($\mathcal{S}_\theta = 18$)
OLS	1.0092×10^{-7}	6.6537×10^{-7}
UOTLS	5.7140×10^{-4}	3.8823×10^{3}
SOTLS	1.2709×10^{6}	1.9371×10^{5}

Table IX presents the MSE's of OLS, WLS and EWLS methods for $N = 3 \times 10^6$. It can be observed from this table that both WLS and EWLS methods outperform the OLS. Moreover, EWLS slightly improves the quality of the results.

TABLE IX
MSE OF ESTIMATED θ FOR OLS, WLS AND EWLS WITH IT OF CLASS 1 AND $N = 3 \times 10^6$

Line	Coaxial	Non coaxial
$\mathcal{S}_\theta$	15	18
OLS	1.0092×10^{-7}	6.6537×10^{-7}
WLS	6.2253×10^{-8}	6.4033×10^{-7}
EWLS	5.2181×10^{-8}	6.2626×10^{-7}

In Figure 6, we show the evolution of the average relative error as a function of the number of samples, N, for OLS, WLS, and WTLS (ML) methods. It can be observed from this figure that (1) all the estimation methods improve the quality of the estimation with the number of samples and (2) all the estimation methods tend to have similar accuracy with a large number of samples. This shows that the proposed estimation methods are consistent. Furthermore, to show the robustness of these estimation methods, we analyzed the variance of the estimation methods as a function of the number of samples. The variance of each component of the parameter vector is different. Therefore, in each case, we choose the component with the maximum variance which is representative of the worst-case performance of the estimation method. In Fig. 7, we plot this maximum standard deviation as a function of the number of samples. It can be observed from this figure that (1) variances decrease with the increase in the number of samples for all estimation methods and (2) all the estimation methods have similar performance in terms of variance.

We expect the WTLS method to outperform the other methods in terms of estimation accuracy, as the likelihood function of WTLS corresponds to the true statistical model for data generation. However, from the plots, we observe that this is not always the case. This can be due to multiple factors including (1) the fact that there is no guarantee that the solution to a non-convex optimization problem returned by a numerical solver is the global optimum of the problem, (2) for a finite number of samples, there is no guarantee of the superiority of the ML estimate over other estimates, and (3) in the EIV model

the effective parameter space increases at the same rate as the number of samples; unlike with the standard least-squares models.

In Table X, we compare the estimation methods in terms of computation time for different sample sizes. It can be observed that although the complexity of each method increases linearly with the number of samples, the OLS outperforms the other estimation methods in terms of computation time. This is because the both the WLS and WTLS methods require computation of noise covariance matrices and the WTLS also requires solving a non-convex optimization problem. In the rest of this section, we only show results obtained from the WLS method as this method provides the most accurate estimates of the parameters within reasonable computation time.

TABLE X
AVERAGE COMPUTING TIME (IN SECONDS) OF ESTIMATION METHODS

Number of samples	WLS	OLS	WTLS
10^2	0.02	0.008	1.38
10^3	0.21	0.013	15.9
10^4	1.9	0.021	165
10^5	19	0.15	–
10^6	267	2.7	–

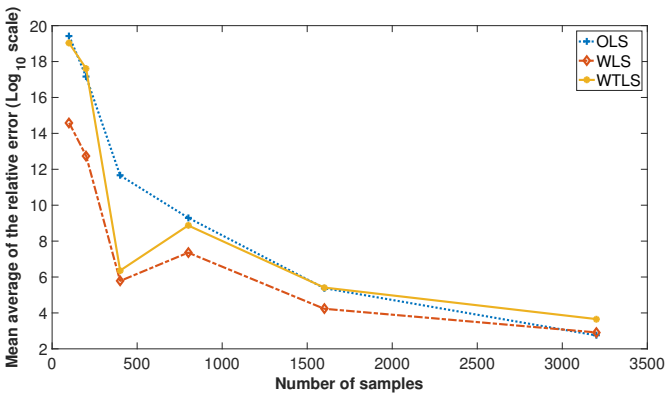

Fig. 6. Average relative error evolution as a function of the number of samples N.

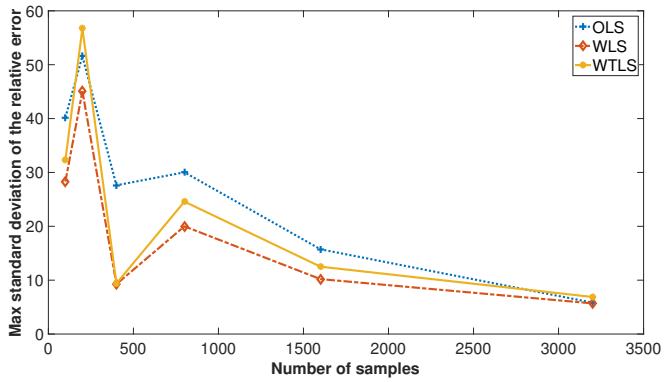

Fig. 7. Evolution of standard deviation of the relative error as a function of the number of samples N.

A more detailed evaluation of the performance of the WLS method with $N = 3 \times 10^6$ is presented in Table XI for both the non-coaxial and coaxial HV lines with $\mathcal{S}_\theta = 18$ and $\mathcal{S}_\theta = 15$, respectively. As described previously, since the actual number of different quantities to estimate is 6 or 5, we average the errors corresponding those components of the (18 or 15 dimensional) parameter vector which measure the same quantity. This helps us to present the results more compactly. We note that the errors are less for the non-coaxial line. This is again due to the fact that the parameters for the non-coaxial line have homogeneous magnitude, whereas for the coaxial line the parameter values are more heterogeneous.

TABLE XI
RELATIVE ERROR FOR EACH COMPONENT OF θ FOR TWO DIFFERENT LINES AND TWO EXTREME CLASSES OF IT.

Relative errors	Coaxial ($\mathcal{S}_\theta = 15$)		Non-coaxial ($\mathcal{S}_\theta = 18$)	
	0.1 IT	1 IT	0.1 IT	1 IT
e_{θ_1}	28	59	2.8	12
e_{θ_2}	17	38	1.1	7.9
e_{θ_3}	58	120	8.1	25
e_{θ_4}	64	160	2.8	19
e_{θ_5}	0.004	0.01	24	25
e_{θ_6}	–	–	180	190

We now use the fact that the lines are fully transposed, which enables us to model them with parameter vectors of size $\mathcal{S}_\theta = 5$ or $\mathcal{S}_\theta = 6$. Using this smaller parameter space, we evaluate the accuracy of the WLS method in Table XII. We observe that the errors reduce significantly in comparison to the previous case (with larger parameter space). This implies that it is always better to use side information, if available, as it reduces the parameter space and considerably improves the accuracy of the estimates.

TABLE XII
RELATIVE ERROR FOR EACH COMPONENT OF θ FOR TWO DIFFERENT LINES WITH REDUCED $\mathcal{S}_\theta$ AND TWO EXTREME CLASSES OF IT.

Relative errors	Coaxial ($\mathcal{S}_\theta = 5$)		Non-coaxial ($\mathcal{S}_\theta = 6$)	
	0.1 IT	1 IT	0.1 IT	1 IT
e_{θ_1}	1.4	16	0.19	2.4
e_{θ_2}	2.2	6.3	0.17	0.87
e_{θ_3}	13	48	1.9	7.7
e_{θ_4}	18	54	0.73	3.1
e_{θ_5}	0.0033	0.01	17	25
e_{θ_6}	–	–	130	190

C. Comparison with existing approaches

We compare our method with existing approaches in [23] and [24]. In [23], OLS estimation using equations derived from an admittance matrix model of the line is proposed. In [24], the same objective function is used, as in [23], but with additional constraints on the ranges of the parameters. Table XIII presents a comparison of the relative errors obtained by the method proposed in [23] and our method. We observe that the method proposed in [23] has significantly higher relative errors. Even for the IT class with the smallest error, the results approach 100% of relative error. Indeed, the results of Table XIII are very similar to those obtained by the Y-line model. Di shi *et*

al in their work also noticed the poor performance of their methods for short TLs.

TABLE XIII
RELATIVE ERRORS OBTAINED WITH THE ESTIMATION METHOD USED IN [23] FOR $N = 3 \times 10^6$

Relative errors	Our Method		Method of [23]	
	0.1 IT	1 IT	0.1 IT	1 IT
$e_{\theta_1^{\mathbf{Y}}}$	4.0	7.2	76	99
$e_{\theta_2^{\mathbf{Y}}}$	14	21	62	99
$e_{\theta_3^{\mathbf{Y}}}$	1.8	2.8	77	99
$e_{\theta_4^{\mathbf{Y}}}$	5.5	7.7	61	99
$e_{\theta_5^{\mathbf{Y}}}$	24	25	240	590
$e_{\theta_6^{\mathbf{Y}}}$	180	190	6900	2700

D. Supplementary test system: Medium Voltage Transmission Lines

In order to further validate the WLS estimation method presented in this paper, we perform experiments on another test system which line parameters are chosen to coincide with realistic values of an overhead transposed Medium Voltage (MV) transmission lines. The table XIV provides the T-line model parameters values of the two lines. It can be observed from Table XV that our method performs well on MV lines. As expected the line impedance parameters are better approximated than the shunt parameters because of the bigger energy loss associated to these quantity. Moreover we observe that for these parameters, the estimation method is able to perform quiet well even when there is no explicit hypothesis on the transposition of the line.

TABLE XIV
TRUE VALUE OF THE PARAMETERS OF THE OVERHEAD TRANSPOSED MV TRANSMISSION LINE.

$\theta_1^{\mathbf{T}}$	4.3×10^{-1}
$\theta_{2^{\mathbf{T}}}$	3.5
$\theta_3^{\mathbf{T}}$	0
$\theta_4^{\mathbf{T}}$	1.4×10^{-1}
$\theta_5^{\mathbf{T}}$	1.3×10^{-5}
$\theta_6^{\mathbf{T}}$	-3.7×10^{-6}

TABLE XV
RELATIVE ERROR FOR EACH COMPONENT OF θ OF A MV TL WITH REDUCED AND UNREDUCED $\mathcal{S}_\theta$ AND TWO EXTREME CLASSES OF IT.

Relative errors	$\mathcal{S}_\theta = 6$		$\mathcal{S}_\theta = 18$	
	0.1 IT	1 IT	0.1 IT	1 IT
e_{θ_1}	1.4×10^{-2}	7.7×10^{-2}	1.9×10^{-1}	15
e_{θ_2}	5.0×10^{-4}	2.1×10^{-1}	5.1×10^{-2}	6
e_{θ_3}	–	–	–	–
e_{θ_4}	1.2×10^{-1}	5.4	1.3	150
e_{θ_5}	95	93	150	135
e_{θ_6}	150	140	373	367

V. CONCLUSION

We have presented methods for estimating parameters of three-phase untransposed short transmission lines at the rated system frequency. We have observed that the selection of the line model plays a crucial role in the accuracy of estimation. In particular for short lines, the proposed T-line model is less sensitive to measurement noise and contains more information about the true line parameters than the Y-line model and the Z-line model typically used to estimate parameters of longer lines. We have proposed an accurate noise model based on the specifications of the instrument transformers and the PMUs. The noise covariance matrices, computed by using the proposed model, enable the estimation of the line parameters with high accuracy. We have evaluated the performance of several least-squares based estimation methods on a real data set obtained from a high voltage sub-transmission grid. We have observed that the WLS method and the ML method, which use the noise covariance matrices, yield the most accurate estimates of the line parameters. In terms of computational complexity, however, the OLS method outperforms the WLS method that in turn outperforms the ML method. We observe that the estimates produced by our proposed approach are significantly more accurate than those produced by existing approaches for line parameter estimation.

There are several interesting avenues for future research. We believe that combinations of different line models could give rise to even better and more stable estimates of line parameters. Furthermore, the selection of the proper line model can be automated using machine-learning techniques.

APPENDIX A
DERIVATION OF $\bar{\mathbf{T}}$ AND $\mathbf{H_T}$ IN T-LINE MODEL

We first express (2) in rectangular coordinates as follows:

$$l^s_{\mathbf{T}} = \bar{\mathbf{T}}(\theta^{\mathbf{T}}) l^r_{\mathbf{T}}, \tag{38}$$

where

$$\bar{\mathbf{T}}(\theta^{\mathbf{T}}) = \begin{bmatrix} \mathbf{I} & -\mathcal{R}(\mathbf{Z}_l(\theta^{\mathbf{T}})) & \mathbf{0} & \mathcal{I}(\mathbf{Z}_l(\theta^{\mathbf{T}})) \\ \mathcal{R}(\mathbf{Y}_l(\theta^{\mathbf{T}}) & -\mathbf{I} & -\mathcal{I}(\mathbf{Y}_l(\theta^{\mathbf{T}})) & \mathbf{0} \\ \mathbf{0} & -\mathcal{I}(\mathbf{Z}_l(\theta^{\mathbf{T}})) & \mathbf{I} & -\mathcal{R}(\mathbf{Z}_l(\theta^{\mathbf{T}})) \\ \mathcal{I}(\mathbf{Y}_l(\theta^{\mathbf{T}})) & \mathbf{0} & \mathcal{R}(\mathbf{Y}_l(\theta^{\mathbf{T}}) & -\mathbf{I} \end{bmatrix} \tag{39}$$

Since $\mathbf{H_T} : \mathbb{R}^{12} \to \mathbb{R}^{12\times 24}$ is linear map, we must have for any $l \in \mathbb{R}^{12}$

$$\mathbf{H_T}(l) = [\mathbf{\Omega}_1 l \quad \mathbf{\Omega}_2 l \ldots \mathbf{\Omega}_{24} l],$$

where each $\mathbf{\Omega}_i$, $i = 1:24$, is in $\mathbb{R}^{12\times 12}$. Now to obtain $\mathbf{\Omega}_i$, for $i = 1:24$, we note that we must have $\mathbf{H_T}(l)\theta = \bar{\mathbf{T}}(\theta)l - \gamma_{\mathbf{T}}(l)$ for any $l \in \mathbb{R}^{12}$ and $\theta \in \mathbb{R}^{24}$. Hence, $\mathbf{\Omega}_i$, $i = 1:24$, can be computed as follows: the j^{th} column of $\mathbf{\Omega}_i$ is given by

$$\mathbf{\Omega}_i(:, j) = \left[\bar{\mathbf{T}}(\theta)l - \gamma(l)\right]_{\theta = e_i^{(24)}, l = e_j^{(12)}}.$$

with $e_k^{(r)}$ denoting the k^{th} unit vector in $\mathbb{R}^r$.

APPENDIX B
PARAMETERIZATION OF DIFFERENT LINE MODELS IN SMALLER PARAMETER SPACE

We parameterization used for the T-line model in dimension $\mathcal{S}_\theta = 6$ is given by

$$\mathbf{Y_l}(\theta^{\mathbf{T}}) = j \begin{bmatrix} \theta_5^{\mathbf{T}} & \theta_6^{\mathbf{T}} & \theta_6^{\mathbf{T}} \\ \theta_6^{\mathbf{T}} & \theta_5^{\mathbf{T}} & \theta_6^{\mathbf{T}} \\ \theta_6^{\mathbf{T}} & \theta_6^{\mathbf{T}} & \theta_5^{\mathbf{T}} \end{bmatrix} \tag{40}$$

$$\mathbf{Z_l}(\theta^{\mathbf{T}}) = \begin{bmatrix} \theta_1^{\mathbf{T}} & \theta_3^{\mathbf{T}} & \theta_3^{\mathbf{T}} \\ \theta_3^{\mathbf{T}} & \theta_1^{\mathbf{T}} & \theta_3^{\mathbf{T}} \\ \theta_3^{\mathbf{T}} & \theta_3^{\mathbf{T}} & \theta_1^{\mathbf{T}} \end{bmatrix} + j \begin{bmatrix} \theta_2^{\mathbf{T}} & \theta_4^{\mathbf{T}} & \theta_4^{\mathbf{T}} \\ \theta_4^{\mathbf{T}} & \theta_2^{\mathbf{T}} & \theta_4^{\mathbf{T}} \\ \theta_4^{\mathbf{T}} & \theta_4^{\mathbf{T}} & \theta_2^{\mathbf{T}} \end{bmatrix} \tag{41}$$

For the Y-line model, the parameterization changes from T-line model only in the first four components of the parameter vector and is given as follows:

$$\mathbf{Z_l}^{-1}(\theta^{\mathbf{Y}}) = \begin{bmatrix} \theta_1^{\mathbf{Y}} & \theta_3^{\mathbf{Y}} & \theta_3^{\mathbf{Y}} \\ \theta_3^{\mathbf{Y}} & \theta_1^{\mathbf{Y}} & \theta_3^{\mathbf{Y}} \\ \theta_3^{\mathbf{Y}} & \theta_3^{\mathbf{Y}} & \theta_1^{\mathbf{Y}} \end{bmatrix} + j \begin{bmatrix} \theta_2^{\mathbf{Y}} & \theta_4^{\mathbf{Y}} & \theta_4^{\mathbf{Y}} \\ \theta_4^{\mathbf{Y}} & \theta_2^{\mathbf{Y}} & \theta_4^{\mathbf{Y}} \\ \theta_4^{\mathbf{Y}} & \theta_4^{\mathbf{Y}} & \theta_2^{\mathbf{Y}} \end{bmatrix} \tag{42}$$

For the Z-line model, the parameterization changes from T-line model only in the last two components of the parameter vector and is given as follows:

$$\mathbf{Y_l}^{-1}(\theta^{\mathbf{Z}}) = j \begin{bmatrix} \theta_5^{\mathbf{Z}} & \theta_6^{\mathbf{Z}} & \theta_6^{\mathbf{Z}} \\ \theta_6^{\mathbf{Z}} & \theta_5^{\mathbf{Z}} & \theta_6^{\mathbf{Z}} \\ \theta_6^{\mathbf{Z}} & \theta_6^{\mathbf{Z}} & \theta_5^{\mathbf{Z}} \end{bmatrix} \tag{43}$$

REFERENCES

[1] E. Ghahremani and I. Kamwa, "Local and wide-area pmu-based decentralized dynamic state estimation in multi-machine power systems," *IEEE Transactions on Power Systems*, vol. 31, no. 1, pp. 547–562, 2015.

[2] S. Sarri, M. Paolone, R. Cherkaoui, A. Borghetti, F. Napolitano, and C. A. Nucci, "State estimation of active distribution networks: comparison between WLS and iterated Kalman-filter algorithm integrating PMUs," in *Proceedings of the 3rd IEEE PES ISGT Europe*, pp. 1–8, 2012.

[3] F. Aminifar, M. Shahidehpour, M. Fotuhi-Firuzabad, and S. Kamalinia, "Power system dynamic state estimation with synchronized phasor measurements," *IEEE Transactions on Instrumentation and Measurement*, vol. 63, pp. 352–363, Feb 2014.

[4] A. Bernstein, L. Reyes-Chamorro, J.-Y. Le Boudec, and M. Paolone, "A composable method for real-time control of active distribution networks with explicit power setpoints. part I: Framework," *Electric Power Systems Research*, vol. 125, pp. 254–264, 2015.

[5] A. Borghetti, M. Bosetti, S. Grillo, S. Massucco, C. A. Nucci, M. Paolone, and F. Silvestro, "Short-term scheduling and control of active distribution systems with high penetration of renewable resources," *IEEE Systems Journal*, vol. 4, no. 3, pp. 313–322, 2010.

[6] L. F. Ochoa, C. J. Dent, and G. P. Harrison, "Distribution network capacity assessment: Variable DG and active networks," *IEEE Transactions on Power Systems*, vol. 25, no. 1, pp. 87–95, 2010.

[7] K. Christakou, J.-Y. LeBoudec, M. Paolone, and D.-C. Tomozei, "Efficient computation of sensitivity coefficients of node voltages and line currents in unbalanced radial electrical distribution networks," *IEEE Transactions on Smart Grid*, vol. 4, no. 2, pp. 741–750, 2013.

[8] Q. Gemine, E. Karangelos, D. Ernst, and B. Cornélusse, "Active network management: planning under uncertainty for exploiting load modulation," in *Proceedings of the IEEE IREP*, pp. 1–9, 2013.

[9] H. Soleimani Bidgoli, M. Glavic, and T. Van Cutsem, "Real-time corrective control of active distribution networks: validation in future scenarios of a real system," *CIGRE Science and Engineering*, vol. 12, pp. 81–99, 2018.

[10] L. G. Perez and A. J. Urdaneta, "Optimal computation of distance relays second zone timing in a mixed protection scheme with directional overcurrent relays," *IEEE Transactions on Power Delivery*, vol. 16, no. 3, pp. 385–388, 2001.

[11] M. Afifi, H. Sharaf, M. Sayed, and D. Ibrahim, "Comparative study between single-objective and multi-objective optimization approaches for directional overcurrent relays coordination considering different fault locations," in *2019 IEEE Milan PowerTech*, pp. 1–6, IEEE, 2019.

[12] M. Gunawardana and B. Kordi, "Time-domain modeling of transmission line crossing using electromagnetic scattering theory," *IEEE Transactions on Power Delivery*, 2019.

[13] J. D. Glover, M. S. Sarma, and T. Overbye, *Power System Analysis & Design, SI Version*. Cengage Learning, 2012.

[14] A. Egozi, "Subscriber line impedance measurement device and method," Nov. 7 1995. US Patent 5,465,287.

[15] A. Momen, B. K. Johnson, and Y. Chakhchoukh, "Parameters estimation for short line using the least trimmed squares (lts)," in *2019 IEEE Power & Energy Society Innovative Smart Grid Technologies Conference (ISGT)*, pp. 1–4, IEEE, 2019.

[16] R. Puddu, K. Brady, C. Muscas, P. A. Pegoraro, and A. Von Meier, "Pmu-based technique for the estimation of line parameters in three-phase electric distribution grids," in *2018 IEEE 9th International Workshop on Applied Measurements for Power Systems (AMPS)*, pp. 1–5, IEEE, 2018.

[17] K. Dasgupta and S. Soman, "Line parameter estimation using phasor measurements by the total least squares approach," in *Proceedings of IEEE PES*, pp. 1–5, 2013.

[18] X. Zhao, H. Zhou, D. Shi, H. Zhao, C. Jing, and C. Jones, "On-line PMU-based transmission line parameter identification," *CSEE Journal of Power and Energy Systems*, vol. 1, no. 2, pp. 68–74, 2015.

[19] D. Shi, D. J. Tylavsky, and N. Logic, "An adaptive method for detection and correction of errors in PMU measurements," *IEEE Transactions on Smart Grid*, vol. 3, no. 4, pp. 1575–1583, 2012.

[20] D. Shi, D. J. Tylavsky, N. Logic, and K. M. Koellner, "Identification of short transmission-line parameters from synchrophasor measurements," in *Proceedings of IEEE NAPS*, pp. 1–8, 2008.

[21] P. A. Pegoraro, K. Brady, P. Castello, C. Muscas, and A. von Meier, "Line impedance estimation based on synchrophasor measurements for power distribution systems," *IEEE Transactions on Instrumentation and Measurement*, vol. PP, no. 99, pp. 1–12, 2018.

[22] D. Ritzmann, J. Rens, P. S. Wright, W. Holderbaum, and B. Potter, "A novel approach to noninvasive measurement of overhead line impedance parameters," *IEEE Transactions on Instrumentation and Measurement*, vol. 66, pp. 1155–1163, June 2017.

[23] D. Shi, D. J. Tylavsky, K. M. Koellner, N. Logic, and D. E. Wheeler, "Transmission line parameter identification using PMU measurements," *International Transactions on Electrical Energy Systems*, vol. 21, no. 4, pp. 1574–1588, 2011.

[24] H. Zhou, X. Zhao, D. Shi, H. Zhao, and C. Jing, "Transmission line sequence impedances identification using PMU measurements," *Journal of Energy and Power Engineering*, vol. 9, pp. 214–221, 2015.

[25] V. Milojevic, S. Calija, G. Rietveld, M. V. Acanski, and D. Colangelo, "Utilization of PMU measurements for three-phase line parameter estimation in power systems," *IEEE Transactions on Instrumentation and Measurement*, vol. PP, no. 99, pp. 1–10, 2018.

[26] C. Mishra, V. A. Centeno, and A. Pal, "Kalman-filter based recursive regression for three-phase line parameter estimation using synchrophasor measurements," in *Proceedings of 2015 IEEE Power Energy Society General Meeting*, pp. 1–5, July 2015.

[27] S. Azizi, M. Sanaye-Pasand, and M. Paolone, "Locating faults on untransposed, meshed transmission networks using a limited number of synchrophasor measurements," *IEEE Transactions on Power Systems*, vol. 31, no. 6, pp. 4462 – 4472, 2016.

[28] C. R. Paul, *Analysis of multiconductor transmission lines*. John Wiley & Sons, 2008.

[29] M. Paolone, J.-Y. Le Boudec, S. Sarri, and L. Zanni, "Static and recursive pmu-based state estimation processes for transmission and distribution power grids," *Advanced Techniques for Power System Modeling, Control and Stability Analysis*, pp. 189–239, 2015.

[30] S. Sarri, *Methods and Performance Assessment of PMU-based Real-Time State Estimation of Active Distribution Networks*. EPFL, 2016.

[31] D. Lerro and Y. Bar-Shalom, "Tracking with debiased consistent converted measurements versus EKF," *IEEE transactions on aerospace and electronic systems*, vol. 29, no. 3, pp. 1015–1022, 1993.
[32] I. Markovsky and S. V. Huffel, "Overview of total least-squares methods," *Signal Processing*, vol. 87, no. 10, pp. 2283 – 2302, 2007.
[33] S. Van Huffel and J. Vandewalle, *The total least squares problem: computational aspects and analysis*. SIAM, 1991.